Received: 25 September 2023 | Accepted: 18 January 2024

DOI: 10.1002/vzj2.20317

Vadose Zone Journal

ORIGINAL ARTICLE

Special Section: Tribute to Rien van Genuchten, Recipient of the 2023 Wolf Prize for Agriculture

Hydro-pedo-transfer-functions expressing drought and memory effects on pine tree growth

Gerd Wessolek[1] | **Winfried Riek**[2] | **Klaus Bohne**[3]

[1]Institute of Ecology, Technical University of Berlin, Berlin, Germany

[2]Faculty of Forest and Environment, Eberswalde University for Sustainable Development (HNEE), Eberswalde, Germany

[3]Department of Soil Science, University of Rostock, Rostock, Germany

Correspondence
Gerd Wessolek, Institute of Ecology, Technical University of Berlin, Berlin, Germany.
Email: wessolekgerd@gmail.com

Assigned to Associate Editor XiaoYan Li.

Funding information
German research foundation (DFG); Federal Ministry of Education and Research, Germany (BMBF)

Abstract

Over the last 30 years, the impact of climate change in Berlin, Germany, has manifested in the form of reduced summer rainfall, elevated temperatures, and a notable rise in the frequency of days with temperatures surpassing 30°C. All of them are leading to a decreasing water supply and increasing risk of drought. Various field, laboratory, and numerical simulation studies have been done for deriving information on long-term potential and actual evapotranspiration, water stress during the vegetation period (April–September), and tree ring growth of various pine tree stands in Berlin. Data analysis highlights periodical climate patterns and complex interactions between drought, water supply, and plant growth. Annual tree ring growth is not only related to the actual weather conditions but also to the past climate years. With decreasing water supply, this kind of drought memory effect increases up to 5 years into the past. For Berlin's climate, it is noteworthy that late summer, particularly the water stress in August, represents the most sensitive indicator for tree ring growth. For regionalization purposes, long-term numerical simulations were done to derive hydro-pedo-transfer-functions (HPTFs) predicting the water stress coefficient of the growing season ($E_{act\text{-}s}/E_{pot\text{-}s}$). They only need easily available information such as soil texture, climate water balance, and groundwater depth. Two HPTFs were successfully tested and can be easily applied by geo-information systems. However, for other climate regions and tree species, HPTFs need to be adapted.

1 | INTRODUCTION

Forests are key elements of terrestrial ecosystems, playing a crucial role in atmospheric cooling, carbon storage, biogeochemical cycles, and the provision of essential goods and services to human populations.

The world's forests face substantial challenges due to climate change, marked by prolonged drought periods, particularly in recent decades (Scharnweber et al., 2020; Spiecker et al., 2023). Because climate change in eastern parts of Germany results in high water deficiency, especially on sites with a deep groundwater table, water supply (WS) became the most relevant factor for tree ring growth and tree health (Bauwe et al., 2015; Cailleret et al., 2017). These aspects are part of the actual discussion on tree species stability and adapting forest management concepts, as done recently by Altieri et al. (2023), Leuschner et al. (2023), and Vacek et al. (2023). However, the consistency of climate relationships with tree growth

Abbreviations: AWC, available water capacity; CWB, climatic water balance; FAO, Food and Agriculture Organization; HPTF, hydro-pedo-transfer-functions; SOM, soil organic matter; TDR, time domain reflectometry; TRW, tree ring width (1/100 mm); WS, water supply; WSC, water stress coefficient.

in terms of direction, duration, and timing is not uniform across space, time, and tree species. The underlying processes responsible for these observed relationships are poorly understood, which hampers our ability to predict future changes in tree growth (Guillemot et al., 2017; Hacket-Pain et al., 2016). A significant contributor to this uncertainty lies in the mechanisms leading to time-lagged effects of climate on tree growth (Hacket-Pain et al., 2015; Peltier et al., 2018; Veuillen et al., 2023). This paper is motivated to address the abovementioned aspects with special regard to WS and drought memory effects on tree ring growth of pine tree stands in the dry region of Berlin, Germany.

In Berlin, since 1984, various field, laboratory, and numerical investigations with respect to different soil hydraulic topics have been done for various pine stands. Most of them are growing on groundwater distant sandy soils, partly on loamy sands, and some are gleyic sandy soils with a shallow groundwater table (<1.5m).

In our previous studies (Greiffenhagen et al., 2006; Riek et al., 1994; Wessolek et al., 2008), we already reported in detail about soil hydraulic properties of forest floor horizons, time domain reflectometry (TDR)-soil moisture, and tensiometer measurements for balancing water budget, modeling soil water dynamic, as well as water repellency occurrence, and preferential flow phenomena. Based on these field and simulation experiences, one can suspect a relationship between plant WS, evapotranspiration, and tree growth, as it first was described by Riek et al. (1995a, 1995b, 1995c).

This contribution focuses on the long-term modeling (spanning >100 years) and analysis of climate impacts on evapotranspiration and water stress coefficients (WSCs), incorporating memory effects on tree ring growth of typical pine stands. For this, tree ring width (TRW) patterns were analyzed and combined with WSC predictions for various time spans. To establish a practical framework suitable for geo-information systems applications, and to enhance the transferability of scientific findings, two hydro-pedo-transfer-functions (HPTFs) were developed for predicting WSC. Results were compared with the outcomes of a calibrated soil–vegetation–atmosphere–transpiration (SVAT) model as a referee.

Core Ideas

- Effects of climate change on water supply of pine trees on sandy soils in Central Europe were studied.
- Tree ring growth was explained using the ratio of actual and potential evapotranspiration predictions.
- Memory effects of drought on tree ring width were studied.
- Growth-effective periods within the vegetation period were evaluated.
- Hydro-pedo-transfer-functions expressing water stress coefficient using easily available site information for geo-information systems-applications were derived.

2 | MATERIALS AND METHODS

2.1 | Site conditions and experimental areas

Since 1984, field investigations have been done on 10 pine stands, growing in different districts of Berlin, Germany (Table 1). Dominant soil texture is fine sandy soil with the corresponding soil types Haplic Arenosol and Podsolic brown soil. Forest floor horizons vary from 2 to 8 cm thickness. The plant available soil water in the rooted soil depth of 0.8 m up to 1.5 m varies between 90 and 150 mm. Depth of the groundwater for most of the pine stands is >30 m below surface, hence irrelevant for the WS of the stocks. Only the pine stand in Berlin Spandau (SP 43) is influenced by a shallow groundwater table in <2.0 m depth. Table 1 gives an overview of all sampled sites with tree characteristics such as age, tree diameter in 1.5-m height, and circular area, which is defined as the mean tree area per 10,000 m^2. In average, 10–15 trees with similar height and diameter per stand have been analyzed for tree ring measurements and site conditions. The tree age differs between 90 and 155 years, with height of the trees is up to 49 m.

The ground vegetation mostly consists of wavy hair grass and moss. Locations are characterized by a continental climate with comparatively uniformly distributed precipitation. In long-term annual average, the precipitation is 577 mm, potential evapotranspiration is 620 mm, and air temperature is 8.9°C. Dry summer periods usually occur in May, leading to severe water deficiency situations for the pine stand already at the beginning of the vegetation period. Figure 1 gives an impression of a typical pine stand of the Grunewald Forest, on which most field experiments and simulation studies were done. The experimental area contains four measuring plots, each instrumented with tensiometer and TDR probes up to 300-cm depth, all connected with a data logger. Details of the measuring technique, equipments used for balancing water budget, and SVAT-model calibrations are given in Rakei (1991), Greiffenhagen et al. (2006), and Wessolek et al. (2021).

2.2 | Analyzing soil hydraulics, evapotranspiration, and water stress (E_{act}/E_{pot})

2.2.1 | Water characteristics

Both mineral soil and forest floor horizons were horizon-wise sampled in spring by means of ten 100 cm^3 cylinders.

TABLE 1 Forest stands and pine tree information.

Site name	Berlin district	Stand no.	Tree age	Number of trees analyzed	Tree height (m)	Tree diameter (cm)	Circular area (m^2 ha^{-1})
TE69	Tegel	69	155	15	28	48	28.5
TE74	Tegel	74	110	15	24	41	28.8
SP43	Spandau	43	135	15	22	39	31.5
SP92	Gatow	92	110	15	21	31	31.5
GR12	Grunewald	12	155	15	23	49	22.1
GR76	Grunewald	76	90	15	20	32	23.3
GR91	Grunewald	91	120	15	21	40	24.9
DÜ60	Düppel	60	140	10	23	43	24.0
DÜ93	Düppel	93	120	15	20	33	26.0
DÜ98	Düppel	98	90	15	23	35	39.2

FIGURE 1 Pine stand of the Grunewald Forest, Berlin, with time domain reflectometry (TDR) probes for measuring continuous soil water content and matrix potential by tensiometers. The white boxes on the left contain the data logger, and on the right, it contains a sandy soil profile.

After re-saturation, the samples were successively dewatered on ceramic plates up to reaching a constant weight. The following dewatering stages, that is, pressure heads were set: pF 1.0, 1.5, 1.8, 2.0, 2.5, 3.0, 3.6, 4.2, and 5.0. Then, the van Genuchten (1980) Equation (1) was fitted to the arithmetic means of water content. The available water capacity (AWC) was related to the soil moisture between pF 1.8 and 4.2 as follows:

$$\theta(h) = \frac{\theta_S - \theta_R}{[1 + (\alpha\, h)^n]^m} + \theta_R \quad (1)$$

where θ is the moisture content (cm^3 cm^{-3}), θ_R is the residual moisture content (cm^3 cm^{-3}), θ_S is the saturation moisture (cm^3 cm^{-3}), h is the pressure head (hPa), α is the fitting parameter (1 cm^{-1}), and n, m, 1 are the van Genuchten parameters (-); $n > 1$ and $m = 1 - 1/n$.

2.2.2 | Hydraulic conductivity

Hydraulic conductivity (K_u) was measured according to Plagge (1991) by means of the steady profile evaporation method and the unsteady instantaneous profile method with three replicates for each soil horizon. The measuring range covers moisture tensions between approximately 20 and 800 hPa. The unsaturated hydraulic conductivity was parameterized according to Mualem (1976) and van Genuchten (1980) as follows:

$$K_u(h) = K_f \cdot \frac{\left\{1 - (\alpha h)^{n-1}\left[1 + (\alpha h)^n\right]^{-m}\right\}^2}{\left[1 + (\alpha h)^n\right]^{m \cdot l}} \quad (2)$$

where K_u is the unsaturated hydraulic conductivity (cm day^{-1}) and K_f is the saturated hydraulic conductivity (cm day^{-1}).

In addition to that, the following parameters were measured for characterizing forest floor horizons and the mineral soil profile: C and N contents by means of a C/N analyzer (Carlo Erba, ANA 1500).

2.3 | Climate

Daily climate records of air temperature, air humidity, radiation, and wind speed from 1950 to 2022 were used from the German climate service (DWD) in Berlin-Dahlem. The station is about 200 m distant from the experimental area of the Grunewald Forest. From this climate station, we include historical, that is, hand written climate data started in 1908–1950, which have been analyzed and published by Riek et al. (1994). This step became necessary in order to reconstruct water stress conditions for the total lifetime of the pine trees that have been planted at the beginning of the 20th century.

2.4 | Soil moisture and tensions

The experimental areas of the Grunewald stands consist of four plots for measuring soil moisture and tensions. Each of them is instrumented by TDR probes (Easy Test, Poland) in 10-cm, 25-cm, 45-cm, 70-cm, 100-cm, 130-cm, 150-cm, 180-cm, 210-cm, 240-cm, 270-cm, and 300-cm depth, each with four replicates. Each TDR probe was calibrated specifically with ethylene glycol and water. Measurements were stored using a data logger and have been used for calibrating the numerical model SVAT, details are described in Section 2.8.

2.5 | Predicting evapotranspiration, photosynthesis, and water stress

Daily climate data of air temperature, air humidity, radiation, wind speed and rainfall have been used from the climate station of the DWD-Station in Berlin-Dahlem to calculate potential Penman Monteith evapotranspiration (E_{pot}), according to the Food and Agriculture Organization (FAO) standard derived by Allen et al. (1998) as follows:

$$E_{\text{pot}} = \frac{\Delta R\text{n}/L + \gamma f(z_{\text{o}},d)u^{0.75}(e_{\text{s}} - e_{\text{a}})}{\Delta + \gamma} \quad (3)$$

where E_{pot} is the potential evapotranspiration (mm) of a grass vegetation of defined height, Δ is the slope of the saturation pressure head function (hPa°C^{-1}), $\gamma$is the psychometric constant (hPa C^{-1}), R_{n} is the net radiation (J m^{-2} day^{-1}), L is the heat of vaporization for 1 mm (J m^{-2} day^{-1}), $f(z_{\text{o}},d)$ is the roughness parameter depending on wind speed and plant height (-), u is the wind speed at 2-m height (measured in open field), e_{s} is the saturation vapor pressure (hPa), and e_{a} is theactual vapor pressure (hPa).

Actual evapotranspiration including interception ($E_{\text{act}} + E_{\text{i}}$) has been calculated using the Penman–Monteith formula as modified by Rijtema (1968) for considering specific plant resistances and soil moisture as follows:

$$E_{\text{act}} + E_i = \frac{\Delta + \gamma}{\Delta + \gamma(1 + f(z_{\text{o}},d)u^{0.75}r)} \left(E_{\text{pot}} - E_{\text{i}}\right) + E_{\text{i}} \quad (4)$$

The plant specific resistances ("r") describing the transport of water through the root and plant are explained in detail by Rijtema (1968) and Wessolek (1989). The interception term (E_{i}) depends on the amount of rainfall, potential evapotranspiration, and soil cover, and the details are explained by DWA (2023). However, for analyzing and relating the water stress conditions to tree ring growth, we did not further consider interception because it is a plant-inactive process.

Under stationary conditions, photosynthesis (P) of the tree (kg ha^{-1}) can be expressed by the following diffusion equation:

$$\text{P} = \frac{\Delta\text{CO}_2}{r'_a + r'_s + r'_m} \quad (5)$$

where ΔCO_2 is the difference between CO_2 concentration in the air and in the plant (needle); r_{a}, r'_a is the diffusion resistance to vapor or CO_2 in the surroundings of the photosynthetic active parts of the tree (= laminar resistance); r_{s}, r'_s is the stomata resistance to water vapor and CO_2; r_{m}, r'_m is the mesophyll resistance to CO_2; and and P is photosynthesis.

Under same environmental conditions, actual transpiration (E_{act}) without interception (E_{i}) can also be described as a diffusion equation:

$$E_{\text{act}} = \frac{\Delta e}{r_a + r_s}. \quad (6)$$

where Δe is the water vapor saturation deficit between leaf, that is, needle and air; r_{a}, r'_a is the diffusion resistance to vapor or CO_2 in the surroundings of the photosynthetic active parts of the tree (= laminar resistance); and r_{s}, r'_s is the stomata resistance to water vapor and CO_2.

Combining Equations (5) and (6), one derives:

$$\frac{E_{act}}{\text{P}} = \frac{\Delta e\left(r'_a + r'_s + r'_m\right)}{\Delta CO_2\left(r_a + r_s\right)} \quad (7)$$

However, under same field conditions, and for daily time steps, CO_2 and the ratio between the plant resistances (r_a, r_s, r_m) levels can be regarded as constant. Thus, we get the following simple equation for predicting the relation of photosynthesis and actual transpiration:

$$\text{P} = A\frac{E_{\text{act}}}{\Delta e} \quad (8)$$

Due to a close relation between Δe and the potential evapotranspiration (E_{pot}), one can use the ratio E_{act}/E_{pot} instead of $E_{act}/\Delta e$ yielding in:

$$P = A\frac{E_{act}}{Epot} \quad (9)$$

The term "A" indicates the "water use efficiency" factor (kg carbon ha^{-1} mm^{-1} hPa^{-1}), which is explained in detail by Feddes et al. (1978).

In the following equation, we simply use the ratio $E_{act\text{-}s}/E_{pot\text{-}s}$ as a WSC describing the WS, that is, deficiency on growing conditions, each year from April 1–September 30:

$$WSC = E_{act-s}/E_{pot-s}\,(-) \quad (10)$$

Potential evapotranspiration can be easily calculated using either by using the Haude's (1955) formula or taking the Penman–Monteith approach (Equation 4). In the past, Haude has been a very familiar, successful, and simple approach for describing potential evapotranspiration in Germany. Main climate input of the Haude formula is simply the water deficit in the air at noon (1 p.m.), which is directly influenced by air temperature, wind speed, and radiation; for more details, the reader can refer to Haude (1955).

Because there is a strong relation between E_{pot} predicted by the Haude approach and the more international established $E_{pot\text{-}Allen}$ formula by Allen et al. (1998), one can easily transform between both approaches for the relevant growing season from April to September by the following Equation (11):

$$E_{pot-Allen} = 1.143 \times E_{pot-Haude}\,(\text{April, 1 till September 30, mm}),\quad r = 0.992 \quad (11)$$

where $E_{pot\text{-}Allen}$ is the potential evapotranspiration according to Allen et al. (1998) and $E_{pot\text{-}Haude}$ is the potential evapotranspiration according to Haude (1955).

Model calibrations use either soil moisture and tensions readings from field studies or lysimeter measurements (Wessolek et al., 2008). Based on tensiometer measurements, it has been observed that a zero-flux plane condition arises during the vegetation period. Consequently, the soil water balance can be resolved without the inclusion of a seepage term, resulting in Equation (12). Measured field data ($E_{act\text{-}m}$) are based on soil moisture readings using TDR probes and hydraulic gradient predictions via tensiometer. During the vegetation period with zero-flux plane conditions ($z = z_n$), $E_{act\text{-}m}$ can be calculated for discreet periods using field measurements of precipitation (P), hydraulic gradients, and soil moisture change versus time (t) and depth (z), yielding in:

$$E_{act-m} = P + \int_{t=1_1}^{t_n}\int_{z=0}^{z_n} \Delta\theta\,(z,t)\,\mathrm{d}z\mathrm{d}t \quad (12)$$

2.6 | Tree ring growth

From each pine stand, 10–15 representative trees with approximately same growth and tree diameter in 1.3-m height were sampled by taking two tree-ring cores per tree using a special tree ring auger, the details are given by von Lührte (1991). Measurements of TRW were done using the ANIOL technique (Aniol, 1983). Dendrochronological standardization of the ring width for filtering biological trends, especially at the beginning of the tree growing period, is described in detail by Cook and Kairiukstis (1990) and Fritts (1976). These techniques were at least used to get standardized, that is, site-specific information of the TRW. Figure 2 shows such normalized tree ring growth, that is, width for all sampled pine stands, as presented in detail by Riek et al. (1994). To avoid biological trends at the early growth stage, tree ring measurements used for this study started in the year 1905 and ends in late 1980s.

2.7 | Simulation models

Two simulations models have been used for this study: First, a conventional SVAT model in order to calculate daily rates of evapotranspiration and percolation (Wessolek et al., 2008), using the following input parameters:

1. daily climate data: precipitation, wind velocity, mean air temperature, mean air humidity, and net radiation;
2. soil hydraulic functions: soil water characteristics, unsaturated hydraulic conductivity, and depth to the groundwater table; and
3. plant data: degree of soil cover, root depth, plant height, and plant specific resistances describing the water transport from soil to the root into the photosynthetic active and transpiring parts.

Additionally, the so-called SWAP (Soil Water Atmosphere Plant) model of Kroes et al. (2017) was taken for numerical modeling and deriving capillary flow rates from the groundwater into the root zone for various climate, groundwater depth, and soil hydraulic conditions. These information have been needed for deriving easily handable pedotransfer functions for sites with a shallow groundwater table, details are described in Section 4.1.

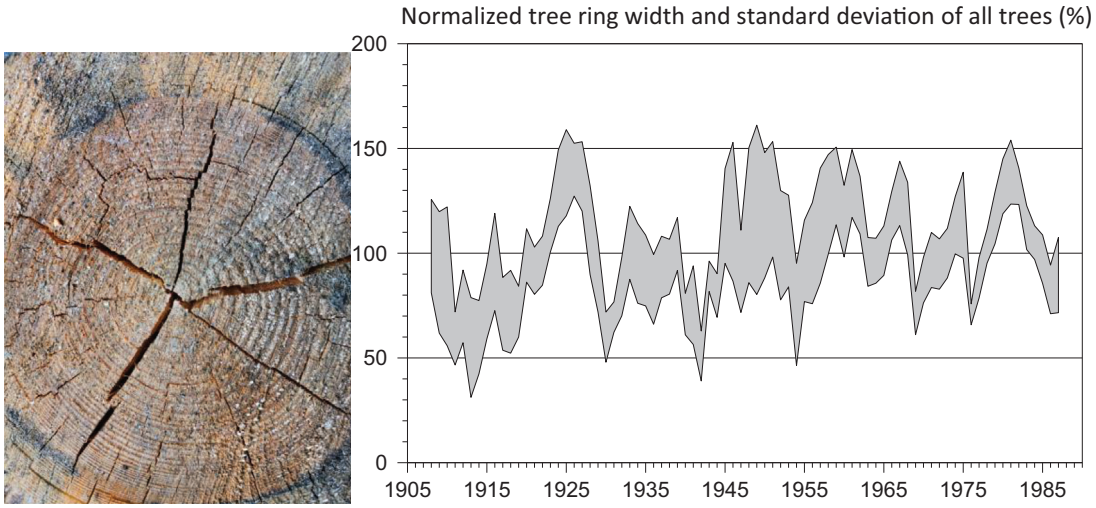

FIGURE 2 Example of a pine tree slice with tree ring widths (left), and normalized long-term mean and standard deviation of all ring widths (right).

2.8 | Model calibration and validation

The SVAT-model calibration utilized measured actual evapotranspiration data ($E_{\text{act-m}}$) obtained from four pine stands in Hannover and Berlin, all situated on fine sandy soils. Among these stands, two have a shallow groundwater table (<1.5 m below the surface), while the other two have a deep groundwater table (>4 m). The calibration process involved adjusting rooting depth and plant resistances to improve the accuracy of simulated soil moisture dynamics and water tensions in comparison to measured data, as outlined in Equation (12). Detailed results are documented in Wessolek (1989), Rakei (1991), Greiffenhagen et al. (2006), and, more recently, in a study on street trees conducted by Wessolek and Kluge (2021).

For an independent validation of the SVAT-model, we conducted a comparison of long-term mean annual values of rainfall minus calculated actual evapotranspiration across a total of 106 German catchment areas. These values were compared with the long-term mean annual total runoff measured by stream flow gauges, and further details can be found in Wessolek et al. (2008). Thus, this paper demonstrates the application of a well-calibrated and validated SVAT model.

2.9 | Statistical analysis

The so-called R-program (Marwick et al., 2017) was used for linear and nonlinear regression analysis, and the software package STATISTICA (Weiß, 2006) for analyzing time series, spectograms, and coherency between data series. With variograms, one can easily predict the time, that is, years in which the actual ring width depends not only on the actual years ($t = 0$), but also of the past years ($t-1$, $t-2$, $t-3$, and $t-n$). Outside this annual time lag h, tree ring growth becomes independent (Riek et al., 1995a). In a variogram, the semivariance γ of TRW depends on the time lag h, describing the annual growing conditions. Semivariance $\gamma\ (h)$ can be predicted as follows (Akin & Siemens, 1988):

$$\gamma\ (h) = \frac{1}{2}\ N\ (h) \sum_{i=1}^{N(h)} \left\{\text{TRW}\left(t_i\right) - \text{TRW}\left(t_{i+h}\right)\right\}^2 \quad (13)$$

where $N(h)$ = number of pairs (TRW(t_i) − TRW ($t_i + h$)) with a time lag $h = 1$ year and TRW(t_i) = tree ring width at time (t_i).

3 | RESULTS AND DISCUSSION

3.1 | Site properties and soil hydraulic characteristics

Table 2 shows exemplarily the soil characteristics of the Berlin-Grunewald Forest. The soil (Podsolic brown soil) is covered on the top by the so-called forest floor horizons, built by litter up to 8 cm thickness. The forest floor horizons are enriched by soil organic matter (SOM) up to 67%, showing a low pH of 3.5 and high cation exchangeable capacity. The dominant soil texture is sand, partly enriched up to 14% with silt in the topsoil, and the clay content is <3%. The mineral soil horizons have a pH of 4–4.5 and are at the top enriched with humus, and SOM is about 6%. The subsoil (C-horizon) can be regarded as a more or less pure sandy soil (<3% silt and clay) with a low SOM.

Table 3 gives some basic information on soil hydraulic properties and MvG parameters used for modeling. The AWC up to an effective rooted soil depth of 1 m is about 110 mm

TABLE 2 Soil characteristics of the Grunewald Forest in Berlin, Germany.

Depth (cm)	Horizon genesis	Texture description	Sand (%)	Silt (%)	Clay	pH ($CaCl_2$)	SOM (g g^{-1})	CEC (mmol kg^{-1})
+8–4.5	Litter	Forest floor	–	–	–	3.5	0.67	183.3
+4.5–0	O_{fh}	Forest floor	–	–	–	3.4	0.51	110.4
0–9	A_{eh}	Fine sand	84.2	13.6	2.2	4.0	0.059	37.3
9–36	Bs_v	Fine sand	90.6	8.3	1.1	4.2	0.015	22.5
36–62	B_v	Fine sand	96.6	2.4	1.0	4.3	0.007	16.5
62–95	C	Fine sand	97.6	2.2	0.2	4.4	0.001	8.5
95–200	C	Fine sand	98.0	2.0	0	4.5	0.001	8.0

Abbreviations: CEC, cation exchange capacity; SOM, soil organic matter.

TABLE 3 Soil hydraulic characteristics.

				Parameters of the water retention function (van Genuchten, 1980)					
Depth (cm)	Bulk density (g cm^{-3})	Field capacity[a] (cm^3 cm^{-3})	AWC[b] (cm^3 cm^{-3})	θ_r (cm^3 cm^{-3})	θ_s (cm^3 cm^{-3})	α (cm^{-1})	n (-)	l (-)	K_{sat} (cm day^{-1})
+8–4.5	0.21	0.343	0.262	0.039	0.887	0.269	1.36	−0.48	1090
+4.5–0	0.34	0.487	0.354	0.080	0.730	0.047	1.38	2.41	445
0–9	1.4	0.154	0.108	0.040	0.417	0.147	1.53	−1.32	243
9–36	1.5	0.130	0.098	0.030	0.447	0.131	1.67	−0.1	545
36–62	1.6	0.072	0.049	0.025	0.383	0.209	1.79	−0.075	813
62–95	1.6	0.053	0.052	0.022	0.374	0.186	1.98	−0.19	830
95–200	1.7	–	–	–	–	–	–	–	–

[a]Field capacity = water content at pF 1.8 ($h = -63$ cm).
[b]AWC = available soil water as a difference between water content at field capacity (pF 1.8) and permanent wilting point (pF 4.2).

and can be classified as "low". K_{sat} is almost high in all horizons.

3.2 | Long-term climate and water balance trends

The general climatic conditions of the northeast German lowlands are characterized by an annual precipitation of 500–660 mm in the transitional area from sub-Atlantic to subcontinental climatic conditions (Table 4). The annual temperature is between 8.2°C and 8.9°C. Dry spells occurring preferably in May cause stressful situations for the forest stands already at the beginning of the vegetation period.

Note that, mean annual precipitation of 578 mm is quite low and is typical for east German climate condition. Note that, 329 mm precipitation on average occurs during the summer season, while in dry (33%) and very dry years (10%), precipitation amounts only 290 and 216 mm, respectively. Mean potential evapotranspiration ($E_{pot\text{-}y}$) is about 600 mm, in dry years (33%, 10%), $E_{pot\text{-}y}$ increases up to 630 and 693 mm, respectively. Thus, annual climate water balance (CWB_y) is slightly negative, while mean CWB_s in summertime (April–September) amounts only −162 mm, and in very dry years <−300 mm (10%). Thus, drought in summertime is a typical phenomenon for these climate conditions, and consequently, mean groundwater recharge under pine stands is quite low (<90 mm), in dry years (33%) often <50 mm, and in very dry years (10%), zero.

To give a first impression of the temporal dynamic during the last 70 years, Figure 3 shows the trend lines by using 10-year moving averages starting in 1950. At the top, middle, and bottom, the annual precipitation (P_y), the annual potential evapotranspiration ($E_{pot\text{-}y}$), and the annual climate water balance ($P_y - E_{pot\text{-}y}$) are shown. While annual precipitation is only slightly decreasing (5%), $E_{pot\text{-}y}$ is increasing significantly by 80 mm since 1990, and climate water balance is drastically decreasing since that time. Next, we are presenting the consequences of these climate induced conditions for the water stress, that is, growing conditions of pine trees.

TABLE 4 Climate and soil water components: average (50%), dry and wet years (33% and 10%), location: Berlin-Dahlem, Germany, period: 1950–2021.

Climate	P_s summer (mm)	P_y year (mm)	$E_{pot\text{-}s}$ summer (mm)	$E_{pot\text{-}y}$ year (mm)	CWB_s summer (mm)	CWB_y year (mm)	GWR year (mm a^{-1})
Median	329	565	473	578	−156	−16	71
Mean	329	578	491	596	−162	−18	86
Dry $p = 33\%$	290	526	519	629	−218	−87	56
Dry $p = 10\%$	216	426	573	693	−326	−221	0
Wet $p = 33\%$	366	629	463	563	−106	51	117
Wet $p = 10\%$	440	729	409	500	2	185	238

Note: Probability of exceedance for P_s: summer precipitation (April till Septmber); P_y: annual precipitation (January till December); $E_{pot\text{-}s}$: potential evapotranspiration of summertime (April till September); $E_{pot\text{-}y}$: annual potential evapotranspiration (January till December); CWB_s: climatic water balance of summertime (April till September); CWB_y: annual climatic water balance (January till December); GWR: groundwater recharge (January till December).

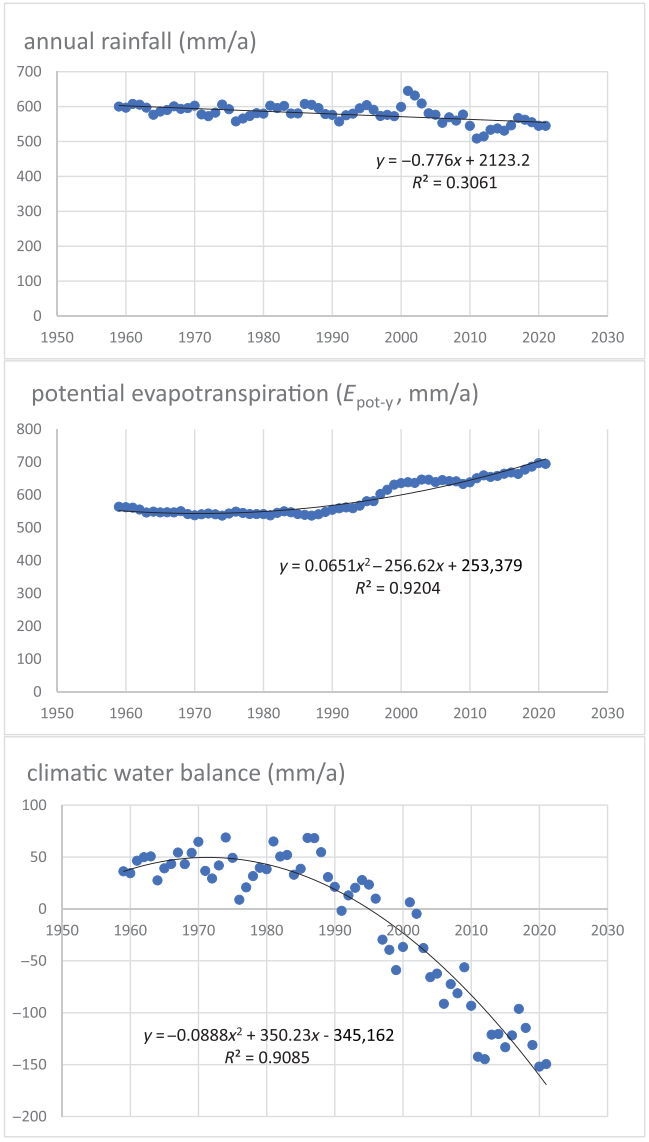

FIGURE 3 Top: Long-term annual precipitation (P_y), middle: annual potential evapotranspiration ($E_{pot\text{-}y}$), bottom: annual climatic water balance ($P_y - E_{pot\text{-}y}$), and trend line: moving averages of 10 years.

3.3 | Long-term actual evapotranspiration and WSCs

Both long-term actual evapotranspiration ($E_{act\text{-}s}$) and WSCs ($E_{act\text{-}s}/E_{pot\text{-}s}$) of the vegetation period, as well as a spectral density function for $E_{act\text{-}s}/E_{pot\text{-}s}$ with period lengths in years (a), were predicted for the Grunewald pine stand (Figure 4).

Long-term actual evapotranspiration during the vegetation period ($E_{act\text{-}s}$) shows only a slight decrease, as depicted by the black line representing 10 years moving averages (Figure 4, top). Additionally, the WSCs ($E_{act\text{-}s}/E_{pot\text{-}s}$) remain nearly constant from 1908 until the early eighties (Figure 4, middle). Subsequently, a pronounced decrease in $E_{act\text{-}s}/E_{pot\text{-}s}$ occurs up to the present, indicating a continuous increase in drought over the past 30 years, as illustrated by the red line. Additionally, results of a time series analysis for the WSCs are presented in Figure 4 (bottom). Frequency patterns occur with period lengths ranging from 2.1 to 7.4 years. However, the biophysiological reasons behind these frequencies, which involve plant adaptations to climate, that is, drought, remain not fully understood. Nevertheless, this suggests for trees developing a certain memory adaptation to recurring water stress situations from the past, influencing their current growth behavior. These aspects shall be deepened in the following section.

3.4 | Tree ring growth and impact of previous years: Memory effects

Exemplarily, Figure 5 shows measured (till 1986) and extrapolated tree ring growth pattern for the Grunewald pine stand, GR76, that has been studied in Riek et al. (1994). The dashed line indicates the moving averages of 4 years, which means that a certain regularity within the growing process can be observed. The extrapolation of the TRW starting 1987 till 2020 has been done using the WSCs of the actual and past vegetation periods as explained next.

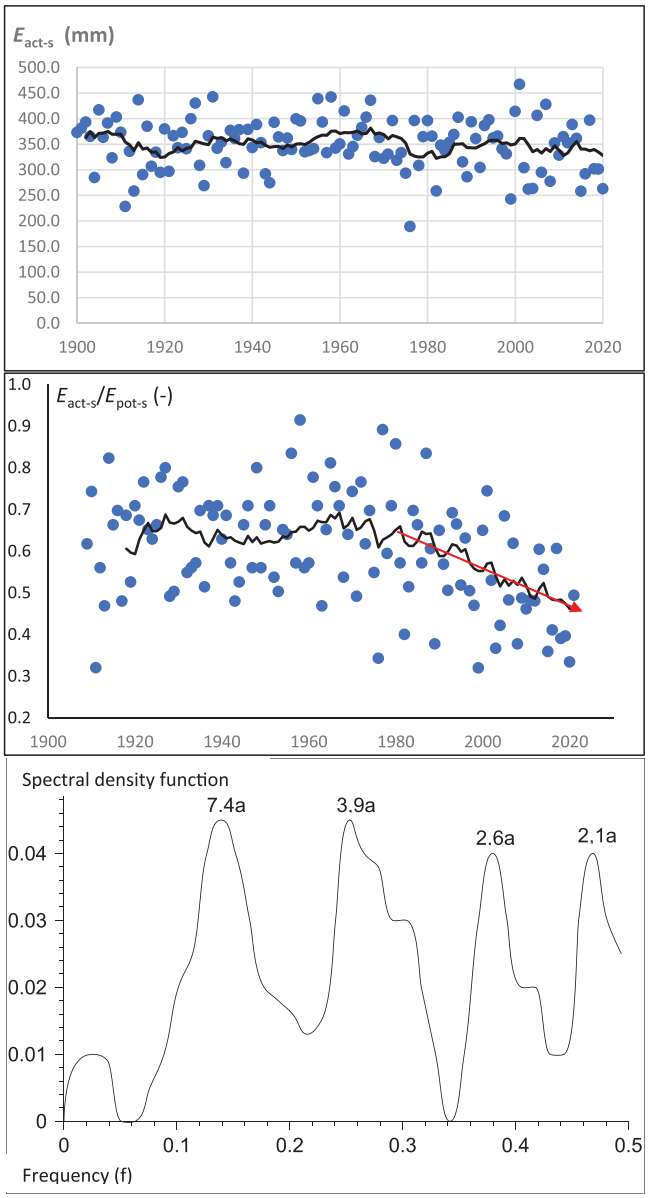

FIGURE 4 Top: long-term actual evapotranspiration (E_{act-s}) of the vegetation period (April 1 till September 30), middle: water stress coefficients (E_{act-s}/E_{pot-s}) of the same period, black line: 10-year averages; bottom: spectral density function (Frequenz, f) expressing long-term period lengths (a) of E_{act-s}/E_{pot-s}.

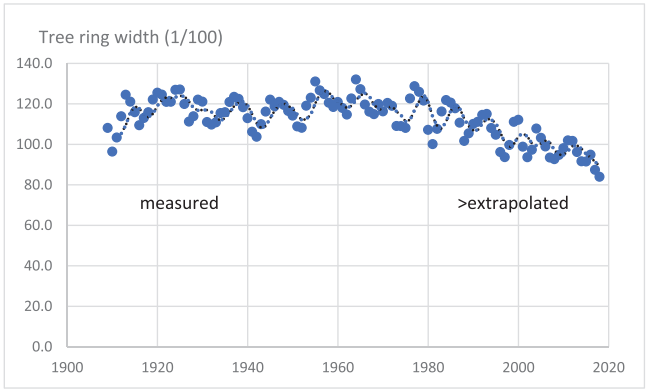

FIGURE 5 Measured till 1986 and extrapolated tree ring width of the Grunewald pine stand (GR76); the dashed line indicates the moving averages of 4 years, modified after Riek et al. (1994).

In order to analyze the time dependency of the tree ring growing process, semivariograms of the annual ring growth versus time have been made; Figure 6 shows the results of four different pine stands. Obviously, the growing process is time dependent, meaning that the actual tree ring growth ($t = 0$) depends not only on the actual climate, that is, WS, but also to the water stress of previous years, up to 5 years. After this time range (g), growing process becomes independent. As a consequence, the annual tree ring growth of various pine stands have been analyzed statistically and set to the water stress conditions of the previous years. Table 5 summarizes this statistical analysis of TRW and WSCs of the vegetation periods (E_{act-s}/E_{pot-s}) for various pine stands in Berlin. For the sandy sites with a deep groundwater table, it is interesting that actual tree ring growth is not only influenced by the water stress of the actual year ($t = 0$), but even more significant from E_{act-s}/E_{pot-s} of the previous years. However, there is one pine stand showing a different behavior: The tree ring growth of the pine stand SP92 has a shallow groundwater table, and the tree ring growth is more or less independent of former climate conditions, that is, E_{act-s}/E_{pot-s}. One can conclude that with an increasing WS, pine tree growing is more stable and less influenced by the past climate years.

In most cases, annual TRW depends on the WS situation of the current and previous 3 years. Thus, actual ring width can be expressed by Equation (14):

$$\begin{aligned} \mathrm{TRW} = {} & 24.38\ E_{act-s}/E_{pot-s(t)} + 50.70\ E_{act-s}/E_{pot-s(t-1)} \\ & + 36.91\ E_{act-s}/E_{pot-s(t-2)} \\ & + 23.86\ E_{act-s}/E_{pot-s(t-3)} + 30.23 \qquad (14) \\ r = {} & 0.698 \end{aligned}$$

The WSC ($E_{act-s}/E_{pot-s(t)}$) of the actual vegetation period explains 19% of the actual tree ring growth, while $E_{act-s}/E_{pot-s(t\ -\ 1)}$ of the previous year explains 37% growth, $E_{act-s}/E_{pot-s(t-2)}$ 2 years ago explains 27% growth, and finally, $E_{act-s}/E_{pot-s(t-3)}$ 3 years ago explains 17% growth.

When analyzing WSCs, the question is raised up: Which of the months within the vegetations period is the most relevant for explaining tree ring growth by water shortage, that is, deficiency? In many years, trees have enough rain and soil water till the end of June. However, in mid of July, soil moisture often drops to a minimum. Thus, severe water deficiency can be pointed out for the whole month of August. Our analysis shows that the WSC of the month August ($E_{act-Aug}/E_{pot-Aug}$)

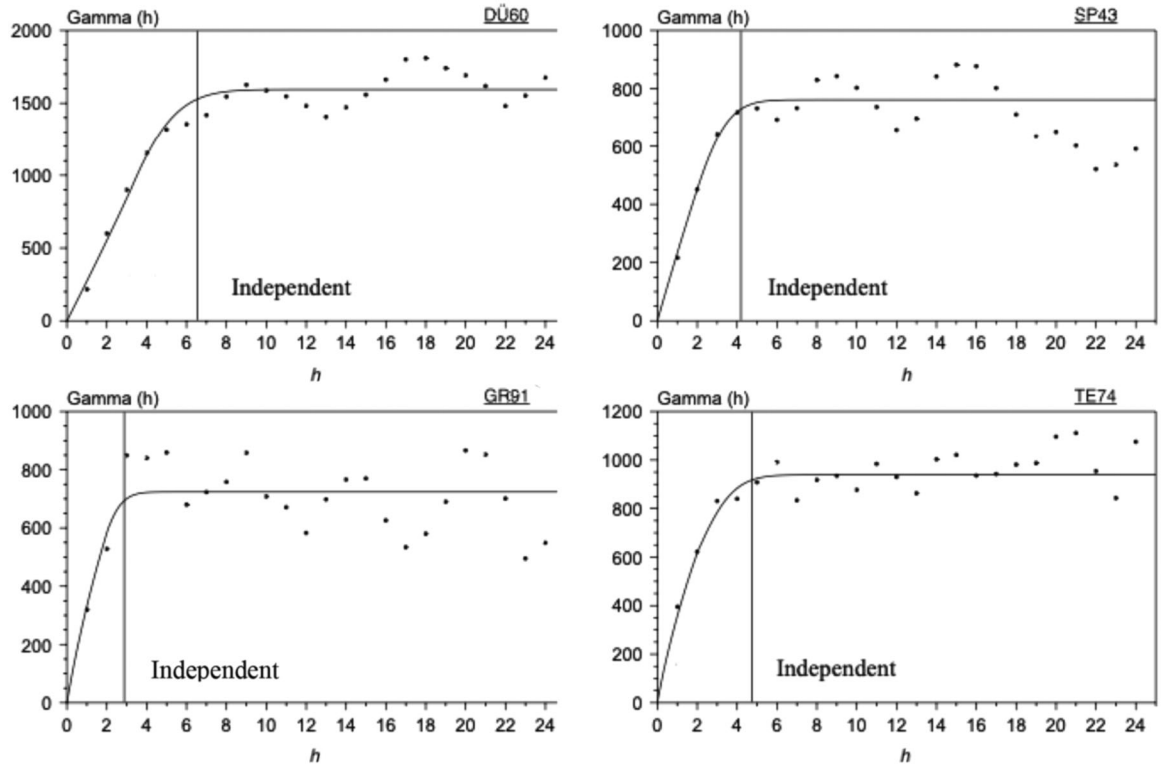

FIGURE 6 Semivariogram analysis of three tree ring width versus time for four typical pine stands in Berlin. The vertical line indicates that tree ring width becomes independent after a certain time period (h = years) passed. This kind of "memory effect" included the following: in the Grunewald pine stand (GR91) a period length of 3 years, in the Spandau stand (SP43) a period of 4 years, and in Düppel (Dü60) a period of 6 years, respectively.

is the most relevant for the sandy soils in Berlin. Thus, the ratio $E_{\text{act-Aug}}/E_{\text{pot-Aug}}$ from August can also be used successfully to reconstruct and interpret changes in WS conditions on tree growth. Similar observations for pine trees were made by Bauwe et al. (2012) and Russ et al. (2017), as well as for spruce trees by Von Wilpert (1990). Figure 7 exemplarily shows for four pine stands that the coefficients for the month of August can successfully be used to re-calculate annual tree ring growth. This month seems, for eastern parts of Germany, the most sensitive indicator of the whole vegetation period. The following equations are examples for the pine stands listed in Table 5:

4 | PEDO-TRANSFER-FUNCTIONS FOR PREDICTING WATER STRESS

HPTFs are well-established tools for regionalizing complex pedo-hydrological information. Unlike numerical models, which require numerous input parameters to address a specific hydrological question, HPTFs demand less easily available data. Thus, they provide comparable results for an entire region, such as a landscape. The following section explains how HTPFS were gained and tested for predicting WSCs by using few site information only.

$$\begin{aligned}
&\text{GR91}: \text{TRW} = 23.98X_t + 52.44\,X_{t-1} + 39.97X_{t-2} + 23.39\,X_{t-3} + 35.10 \quad (r = 0.77)\\
&\text{SP43}: \text{TRW} = 31.61\,X_t + 38.16\,X_{t-1} + 38.87\,X_{t-2} + 29.45\,X_{t-3} + 21.84 \quad (r = 0.74)\\
&\text{DÜ98}: \text{TRW} = 54.99\,X_t + 69.94\,X_{t-1} + 37.70\,X_{t-2} + 30.30\,X_{t-3} + 37.16 \quad (r = 0.79)\\
&\text{DÜ93}: \text{TRW} = 40.27\,X_t + 68.56\,X_{t-1} + 58.29\,X_{t-2} + 41.70\,X_{t-3} + 19.84 \quad (r = 0.79)\\
&(\text{TRW} = \text{annual tree ring width in the year } t\ (1/100\text{ mm});\ X_t = \text{water stress coefficient in August}\\
&\left(E_{\text{act}-\text{Aug}}/E_{\text{pot}-\text{Aug}}\right) \text{ of the current } (t) \text{ and of the previous three years } (t-1,\ t-2,\ t-3).
\end{aligned} \tag{15}$$

TABLE 5 Annual tree ring growth and water stress coefficients ($E_{act\text{-}s}/E_{pot\text{-}s}$) of the actual year ($t = 0$), and previous years for different pine stands in Berlin.

Site name	Soil and groundwater	$E_{act\text{-}s}/E_{pot\text{-}s}$ of $t = 0$	$t - 1$ year	$t - 2$ years	$t - 3$ years	Durbin–Watson	Multiple correlation coefficients
GR76	Sandy soil	*	***	**	*	0.74	0.66**
GR91	No groundwater influence	*	***	**	*	1.04	0.65**
SP43	Sandy soil no groundwater influence	*	**	*	*	0.68	0.57**
DÜ93	Sandy soil	*	**	**	*	0.70	0.56**
DÜ98	No groundwater influence	**	***	*	*	1.15	0.65***
DÜ60	Sandy loamy soil no groundwater influence		*	*	*	0.79	0.51*
TE74	Sandy soil no groundwater influence	*	**	*	*	0.95	0.58**
SP92	Sandy soil with a shallow groundwater		*			0.98	0.32*

Note: Only the site SP92 is influenced by groundwater.
*, **, and *** denote significance at $p < 0.05$, $p < 0.01$, and $p < 0.001$, respectively.

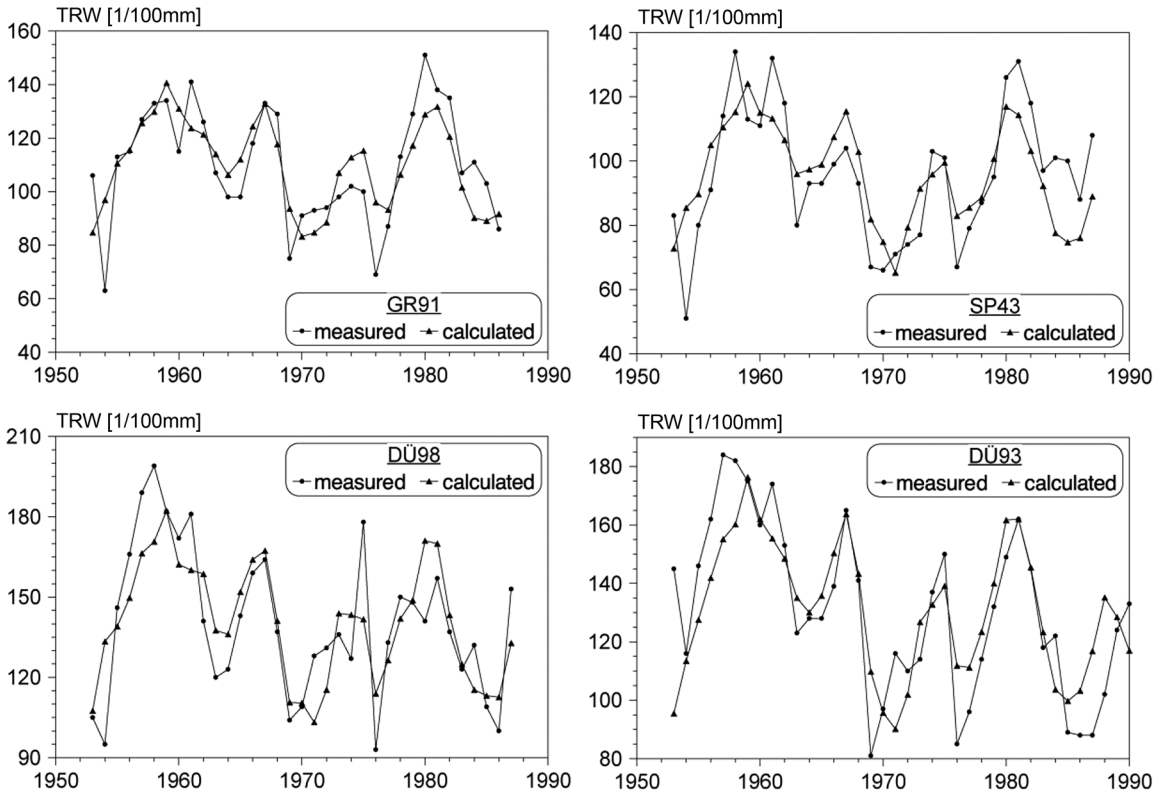

FIGURE 7 Development of tree ring width (TRW) of four typical pine stands in Berlin: Comparison of measured data (dots) and predicted values (triangles) based on water stress coefficients ($E_{act\text{-}Aug}/E_{pot\text{-}Aug}$) of August for the current (t) and previous three years ($t - 1$, $t - 2$, t – 3). Predictions were done using the stand specific Equation (15).

5 | Principles

The ratio of actual to potential evapotranspiration ($E_{act\text{-}s}/E_{pot\text{-}s}$) in the vegetation period depends on both: WS and potential evapotranspiration itself. WS can be easily estimated by half of the (1) soil available water (PAW) in the effective root zone, (2) summer precipitation (P_s), and (3) in case of a shallow groundwater table, by capillary rise (Q_a)

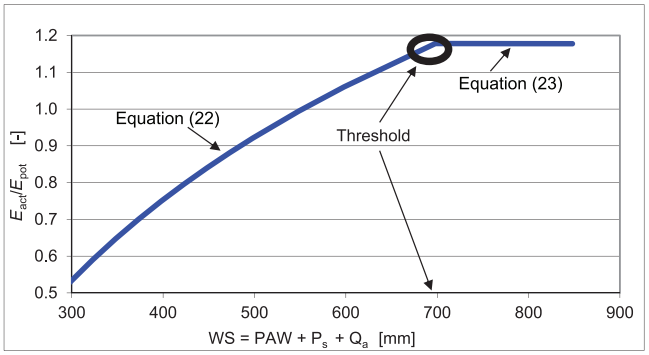

FIGURE 8 Principles of the TUB-BGR approach using a water supply (WS) threshold (Wessolek et al., 2008). PAW, soil available water.

from the groundwater to the root zone, hence:

$$\mathrm{WS} = 0.5\mathrm{PAW} + P_s + Q_a \tag{16}$$

Field measurements show that, in most years, tree roots do not completely extract the soil water during the vegetation period, therefore total, that is, potential PAW was reduced by half of PAW, further information on deriving Q_a are given within the explanations of the HPTFs.

As mentioned before, the WSC can be defined as the ratio of $E_{act\text{-}s}/E_{pot\text{-}s}$ (-), where E_{act_s} and $E_{pot\text{-}s}$ denote the actual and potential evapotranspiration during the summertime (April 1–September 30), respectively. The WSC can characterize the influence of various WS conditions on plant growth.

To obtain a convenient estimation of WSC using easily available site information only, two HPTFs were derived for pine tree stands and compared with daily calculated simulation results using SVAT.

The first HPTF is a very simple approach, just using the ration of WS and $E_{pot\text{-}s}$ by:

$$\mathrm{WSC} = \mathrm{WS}/1.2\,E_{pot-s} \tag{17}$$

in which 1.2 is used as an approximation, considering that potential evapotranspiration for trees is higher than for a grass vegetation because of a higher roughness (DWA, 2023).

The second HPTF picks up the principles of the so-called TUB-BGR approach, first published by Wessolek et al. (2008). The idea behind this model is illustrated in Figure 8.

E_{act}/E_{pot} reaches a certain threshold of WS, in this case 700 mm. Water used for evapotranspiration of the trees is either coming from precipitation, soil pores, or from the groundwater by capillary rise. If WS exceeds 700 mm, water is not anymore a limiting evapotranspiration factor, thus, E_{act} can be easily predict by Equation (18) using E_{pot} only. Please note that E_{act} can surpass E_{pot}, because the original E_{pot} formula has been developed as a standard formula for grassland, while E_{pot} for pine trees is much higher and underlay an increased wind speed resulting finally in a higher roughness, as mentioned before.

The original TUB-BGR equation was slightly modified to calculate pine tree transpiration for the vegetation period only:

$$E_{act-s} = E_{pot-y}\left[1.68\log\left(0.5\,\mathrm{PAW} + P_s + Q_a\right) - 3.53\right] \times \left[0.95\log\left(1/E_{pot-y}\right) + 3.52\right] \tag{18}$$

$$E_{act-s} = E_{pot-y} \times 1.2\,[0.66\log\left(1/E_{pot-y}\right) + 3.52 \tag{19}$$

Since the actual capillary rise (Q_a) from groundwater table depends on both soil hydraulic functions and climate (potential evapotranspiration), soil- and climate-specific limitations of total capillary rise needs to be considered in Equation (20).

First, one needs to calculate soil-specific capillary rise rates: we call them ''potential capillary rise rates'' (Q_{pot}) because they express the potential daily upward flow rates without climatic limitation. Steady-state capillary flow rates can be predicted easily by the Darcy equation:

$$Q_{pot} = -k\left(\frac{\mathrm{d}h}{\mathrm{d}z} + 1\right) \tag{20}$$

where Q_{pot} is the potential capillary rise rate (mm day^{-1}); h is the pressure head (hPa); z is the vertical distance (cm); and k is the soil hydraulic conductivity according to Mualem/van Genuchten (cm day^{-1}).

Integration of Equation (20) yields,

$$\int_{z1}^{z2} dz = \int_{h1}^{h2} \frac{-1}{1 + q/K\,(h)}\mathrm{d}h. \tag{21}$$

Starting at the groundwater table where $h = 0$, one can calculate pressure head profiles with depth, that is, $h(z)$ for various flux values (Q_{pot}). Many authors (e.g., Bloemen, 1980, 1983; Brandyk & Wesseling, 1985; Renger & Strebel, 1980) calculated them by solving Equation (21) numerically for various steady-state pressure heads and distances between the groundwater table and the bottom of the effective root zone. Figure 9 exemplarily shows such capillary rise rates for the soils, for which the HPTFs were developed.

Next, land use specific time (t in days) during which one can expect an active capillary rise is needed.

In Germany, this period takes about 120 days (t) for forests with shallow groundwater tables. Detailed information is given in Ad-Hoc AG Boden (2005). Hence, the maximum annual capillary rise of groundwater (Q_{max}) into the root zone is given by:

$$Q_{max} = Q_{pot} * \mathrm{t} \tag{22}$$

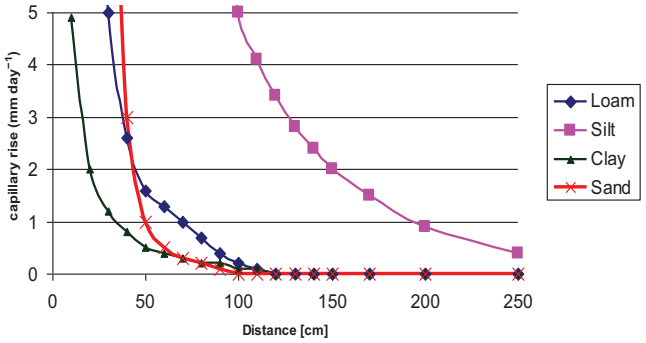

FIGURE 9 Capillary rise rates from the groundwater table to the root zone (= distance) for various soils.

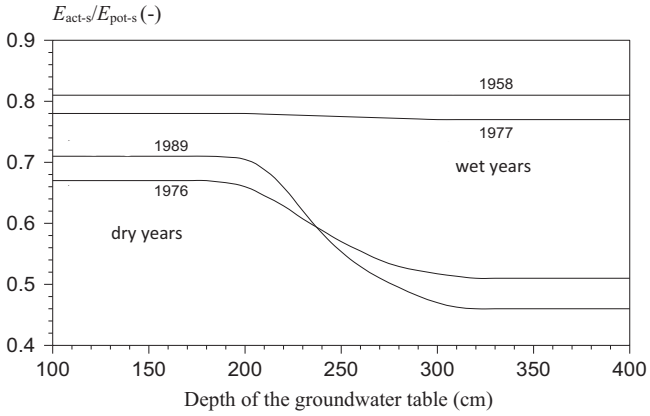

FIGURE 10 $E_{act\text{-}s}/E_{pot\text{-}s}$ (-) as a function of the groundwater depth in dry (1976, 1976), and wet years (1958, 1977) for a sandy soil in Berlin, Germany.

Finally, we consider the upper limit of capillary rise depending solely on climatic conditions. We call this the "climate-controlled annual capillary rise" (Q_{cli}), and it is calculated using a site-specific equation:

$$Q_{cli} = 1.3E_{pot-s} - \left(P_s + 0.5\,AWC\right) \quad (23)$$

where Q_{cli} is the climate-controlled annual capillary rise (mm), $E_{pot\text{-}s}$ is the potential evapotranspiration from April 1 to September 30 (mm) and P_s is the precipitation from April 1 to September 30 (mm).

The empirical coefficient 1.3 in Equation (23) is an expression of methodological differences in the calculation of the potential evapotranspiration in the SVAT model (done with a modified Penman–Monteith-approach) and the FAO grass reference evapotranspiration (as used to generate HPTFs). The coefficient 0.5 in Equation (23) results from field measurements on sites with a shallow groundwater table in which capillary rise into the root zone started when soil water was <50% AWC (Renger & Strebel, 1980).

$E_{pot\text{-}s}$ in Equation (23) can be easily calculated by a simple linear regression equation relating the FAO grass reference evapotranspiration of the summer half-year ($E_{pot\text{-}so}$) to $E_{pot\text{-}y}$ of the entire year ($E_{pot\text{-}y}$). This has been predicted for various long-term climate rows in Germany (Wessolek et al., 2008). A linear regression analysis between $E_{pot\text{-}y}$ and $E_{pot\text{-}s}$ shows a close relationship, the equation for German climate conditions is given as follows:

$$E_{pot-s} = 0.72E_{pot-y} + 48 \qquad \left(r^2 = 0.9451\right) \quad (24)$$

This close correlation is to be expected, since the variables are not independent. However, because the relationship is being used not as an explanation but as a predictor only, the plot is useful and informative.

Among other things, it shows that potential summer evapotranspiration is about 75% of the annual potential evapotranspiration, thus allowing people who need summer half-year values (which are often not available) to estimate them from available annual values (which are usually available). To make a realistic assessment of the actual amount of annual capillary rise (Q_a) needed in the HPTF, three conditions may be distinguished:

if $Q_{cli} < 0$, then $Q_a = 0$
if $Q_{max} > Q_{cli}$, then $Q_a = Q_{cli}$
if $Q_{max} < Q_{cli}$, then $Q_a = Q_{max}$.

5.1 | Scenarios

To assess the suitability and accuracy of the two HPTFs, specific and long-term predictions of $E_{act\text{-}s}/E_{pot\text{-}s}$ were conducted for diverse site conditions and climates. Both the SVAT-model predictions and the results of the two HPTFs were employed for this analysis.

The initial scenario presents $E_{act\text{-}s}/E_{pot\text{-}s}$ under various groundwater depth and climate conditions, specifically for two wet and two dry years (Figure 10). Simulations were conducted on a daily basis for an old pine stand on sandy soil using the SVAT-model. The results exemplify variations in WSCs ranging from 0.45 to >0.8. Interestingly, in wet years, WSC appears relatively independent of groundwater depth, while in dry years, $E_{act\text{-}s}/E_{pot\text{-}s}$ is the lowest for pine stands located on sites with a deep groundwater table. Consequently, these findings lead to the decision to conduct a suitability test for the HPTFs under two distinct site conditions: one with a deep groundwater table and another with a shallow one.

Keeping these climate and groundwater induced WSC variations in mind, both HPTF approaches were tested and compared with the results of the SVAT model, which can be interpreted as a referee. As mentioned before, the HPTFs use the sums of summer precipitation and E_{pot} as input data, while the SVAT predictions are based on daily climate data. The test should answer two questions: (1) can the HPTF recalculate the WSC trend of the past and (2) are the absolute WSC

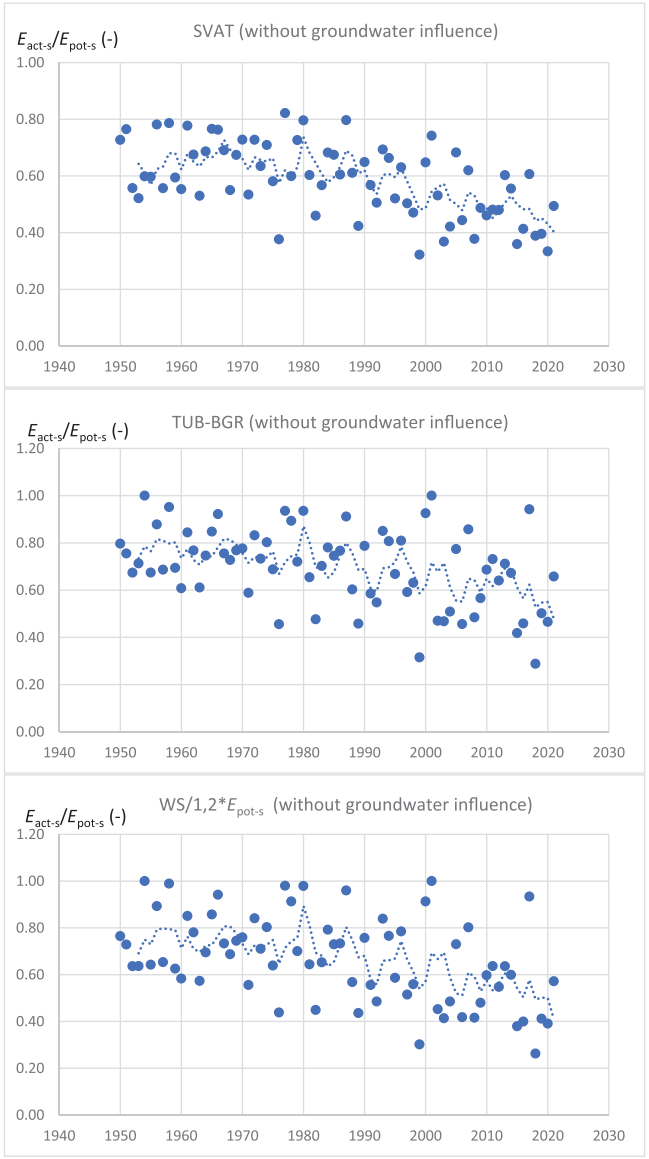

FIGURE 11 E_{act-s}/E_{pot-s} predicted (dots) by the soil–vegetation–atmosphere–transpiration (SVAT)-model (top, referee), the TUB-BGR approach (middle), and expressed by the ratio of WS/1.2*E_{pot-s} (bottom). Dashed-line: 10-year averages. WS, water supply.

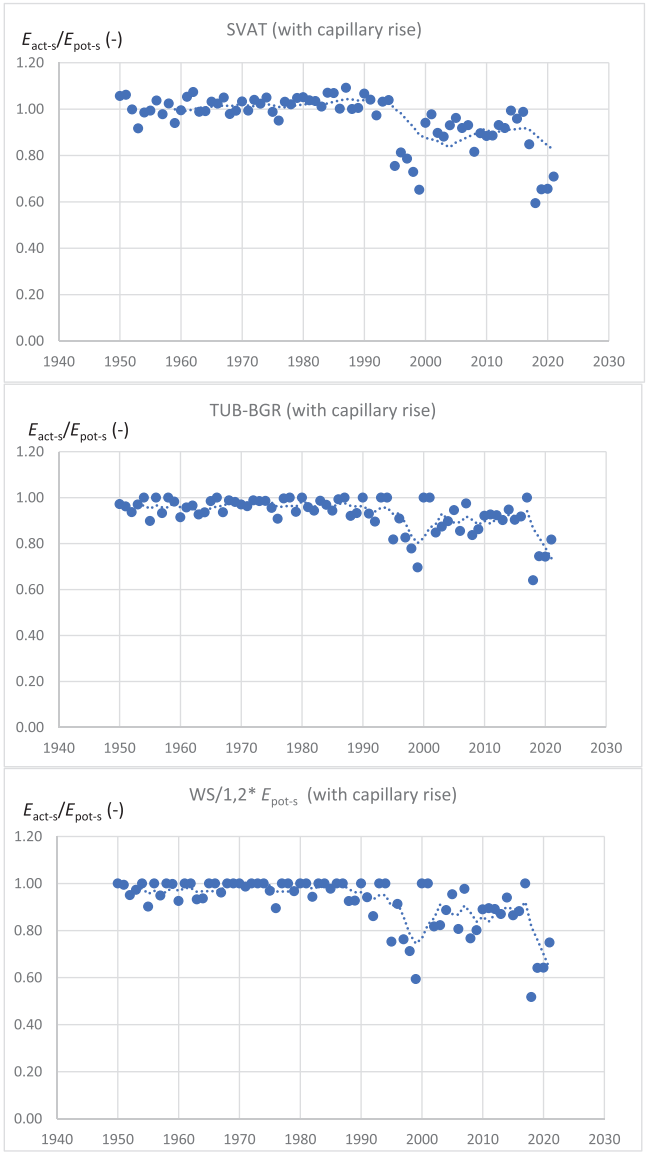

FIGURE 12 E_{act-s}/E_{pot-s} predicted (dots) by the soil–vegetation–atmosphere–transpiration (SVAT)-model (top, referee), the TUB-BGR approach (middle), and expressed by the ratio of WS/1.2*E_{pot-s} (bottom). Dashed-line: 10-year averages. WS, water supply.

values between groundwater distant and groundwater influenced pine stands in the same order of magnitude as those calculated with the SVAT model?

For this test, Berlin climate row from 1950 to 2021 was used to predict WSC for a sandy soil with and without a groundwater influence. Results of these scenarios for an old pine stand are presented in Figure 11 without any groundwater influence and in Figure 12 for the same soil and climate conditions, but with a shallow groundwater table in 1.4-m depth.

All in all, one can point out that both HPTF approaches are well suited to predict WSC for both site conditions, that is, with and without capillary rise. Even more, the trend and shape of decreasing WSC since 1990 could be reconstructed well using both equations. In addition, the absolute values of the WSC predictions are in the same order of magnitude compared to the daily simulation results of the SVAT model.

6 | CONCLUSIONS

Long-term actual evapotranspiration of pine stands with a deep groundwater table in Berlin, Germany, showed slightly decreasing trend since about 30 years, while potential evapotranspiration is strongly increased. Thus, WSCs (WSC

$= E_{act\text{-}s}/E_{pot\text{-}s}$) is dropping from about 0.7 in the past down to actually 0.4, which can be interpreted as a key indicator of climate change, that is, increasing risk of drought. In contrast, pine stands with a shallow groundwater table compensate increasing drought by capillary rise as long as the water table keeps stable and is not falling. TRW is strongly correlated with the WSC during the growing period. Within this time, the month of August is the most relevant indicator for pine tree growing on sandy soils in east Germany.

However, the relation between growth and evapotranspiration depends not only on the water stress conditions of the actual vegetation period, but also on the water stress of the past years. With decreasing WS, this biological memory effect of water deficiency becomes stronger and exceeds up to 5 years. For numerical model developer, it would be a challenge to incorporate such kind of "memory function" in common SVAT models for considering biological feedback mechanism.

Two HPTFs have been derived and successfully tested for predicting WSCs ($E_{act\text{-}s}/E_{pot\text{-}s}$) for various climate and groundwater depth conditions of Berlin by taking easily available site information into account. However, for other climate regions, these HPTF equations certainly have to be adapted.

AUTHOR CONTRIBUTIONS

Gerd Wessolek: Conceptualization; data curation; formal analysis; funding acquisition; investigation; methodology; project administration; resources; software; supervision; validation; visualization; writing—original draft; writing—review and editing. **Winfried Riek**: Conceptualization; data curation; formal analysis; methodology; resources; software; validation; visualization; writing—review and editing. **Klaus Bohne**: Conceptualization; formal analysis; methodology; software; validation; visualization; writing—original draft; writing—review and editing.

ACKNOWLEDGMENTS

This article is dedicated to two colleagues: first, to Prof. Dr Manfred Renger, who passed away in June 2023. Manfred's scientific work in soil physics and soil hydrology at the Technical University Berlin has been unique for the German soil science community. Among others, he introduced and designed easily handable Hydro-Pedo-Transfer-Functions for balancing water budget and crop yield relations. During the time of the "cold war," it was Manfred, who closely cooperated with the Institute of Agrophysics in Lublin, Polen, in designing, testing, and applying new TDR technique and device.

The second person we would like to honor and thank is Prof. Dr Rien van Genuchten. His input in soil physics and designing numerical model tools such as HYDRUS is worldwide unique. The authors are grateful to Rien for cooperating with us many years, especially with the German research group "Interurban" financed by the German research foundation (DFG), and of course for his open mind and friendship. For example, Rien very early encouraged Gerd to investigate in soil and art. We sincerely appreciate the reviewer for their valuable and insightful comments, which have greatly contributed to improving and enhancing our manuscript. Investigations were funded within the Deutsche Forschungsgemeinschaft (DFG) and by the Federal Ministry of Education and Research, Germany (BMBF).

CONFLICT OF INTEREST STATEMENT

The authors declare no conflicts of interest.

ORCID

Gerd Wessolek https://orcid.org/0000-0003-3374-3794

REFERENCES

Ad-Hoc AG Boden. (2005). *Bodenkundliche Kartieranleitung* (5th ed.). Schweizerbart. (In German). https://www.schweizerbart.de/publications/detail/isbn/9783510959204/Bodenkundliche_Kartieranleitung_5_Aufl

Akin, H., & Siemens, H. (1988). *Praktische Geostatistik. Eine Einführung für den Bergbau und die Geowissenschaften*. Springer. (In German).

Allen, R. G., Pereira, L. S., & Raes, D. (1998). *Crop evapotranspiration guidelines for computing crop requirements* (FAO Irrigation and Drainage Paper 56). FAO. http://www.climasouth.eu/sites/default/files/FAO%2056.pdf

Altieri, S., Valor, T., & Battipaglia, G. (2023). Editorial: Forest adaptation to extreme environments and climate changes. *Frontiers in Ecology and Evolution*, *11*, 1230753. https://doi.org/10.3389/fevo.2023.1230753

Aniol, R. W. (1983). Tree-ring analysis using CATRAS. *Dendrochronologia*, *1*, 45–53.

Bauwe, H., Hagemann, M., Kern, R., & Timm, S. (2012). Photorespiration has a dual origin and manifold links to central metabolism. *Current Opinion in Plant Biology*, *15*(3), 269–275. https://doi.org/10.1016/j.pbi.2012.01.008

Bauwe, A., Jurasinski, G., Scharnweber, T., Schröder, C., & Lennartz, B. (2015). Impact of climate change on tree-ring growth of Scots pine, common beech and pedunculate oak in northeastern Germany. *iForest—Biogeosciences and Forestry*, *9*, 1–11. http://www.sisef.it/iforest/contents/?id=ifor1421-008

Bloemen, G. W. (1980). Calculation of steady state capillary rise from the groundwater table in multi-layered soil profiles. *Journal of Plant Nutrition and Soil Science*, *143*(6), 701–719.

Bloemen, G. W. (1983). Calculation of hydraulic conductivities and steady state capillary rise in peat soils from bulk density and solid matter volume. *Journal of Plant Nutrition and Soil Science*, *146*(4), 460–473. https://doi.org/10.1002/jpln.19831460407

Brandyk, T., & Wesseling, J. G. (1985). Steady state capillary rise in some soil profiles. *Journal of Plant Nutrition and Soil Science*, *148*(1), 54–65. https://doi.org/10.1002/jpln.19851480107

Cailleret, M., Jansen, S., Robert, E. M. R., Desoto, L., Aakala, T., Antos, J. A., Beikircher, B., Bigler, C., Bugmann, H., Caccianiga, M., Čada, V., Camarero, J. J., Cherubini, P., Cochard, H., Coyea, M. R., Čufar, K., Das, A. J., Davi, H., Delzon, S., … Martínez-Vilalta, J. (2017). A synthesis of radial growth patterns preceding tree mortality. *Global Change Biology*, *23*(4), 16751690. https://doi.org/10.1111/gcb.13535

Cook, E. R., & Kairiukstis, L. A. (Eds.). (1990). *Methods of dendrochronology—Applications in the environmental sciences*. Springer. https://doi.org/10.1007/978-94-015-7879-0

DWA. (2023). Ermittlung der Verdunstung von Land- und Wasserflächen-Teil 2: Berechnungsverfahren der Landverdunstung (Merkblatt DWA_M 504-2). (In German). https://de.dwa.de/de/regelwerk-news-volltext/berechnungsverfahren-der-landverdunstung-entwurf-merkblatt-dwa-m-504-2.html

Feddes, R. A., Kowalik, P. J., & Zaradny, H. (1978). *Simulation of field water use and crop yield*. Centre for Agricultural Publishing and Documentation. https://edepot.wur.nl/172222

Fritts, H. C. (1976). *Tree rings and climate*. Academic Press. https://doi.org/10.1016/B978-0-12-268450-0.X5001-0

Greiffenhagen, A., Wessolek, G., Facklam, M., Renger, M., & Stoffregen, H. (2006). Hydraulic functions and water repellency of forest floor horizons on sandy soils. *Geoderma*, *132*(1–2), 182–195. https://doi.org/10.1016/j.geoderma.2005.05.006

Guillemot, J., Francois, C., Hmimina, G., Dufrêne, E., Martin-Stpaul, N. K., Soudani, K., Marie, G., Ourcival, J.-M., & Delpierre, N. (2017). Environmental control of carbon allocation matters for modelling forest growth. *New Phytologist*, *214*, 180–193.

Hacket-Pain, A. J., Cavin, L., Friend, A. D., & Jump, A. S. (2016). Consistent limitation of growth by high temperature and low precipitation from range core to southern edge of European beech indicates widespread vulnerability to changing climate. *European Journal of Forest Research*, *135*, 897–909.

Hacket-Pain, A. J., Friend, A. D., Lageard, J. G. A., & Thomas, P. A. (2015). The influence of masting phenomenon on growth-climate relationships in trees: Explaining the influence of previous summers' climate on ring width. *Tree Physiology*, *35*, 319–330.

Haude, W. (1955). *Zur Bestimmung der Verdunstung auf möglichst einfache Weise*. Mitteilungen Deutscher Wetterdienst. (In German).

Kroes, J. G., van Dam, J. C., Bartholomeus, R. P., Groenendijk, P., Heinen, M., Hendriks, R. F. A., Mulder, H. M., Supit, I., & van Walsum, P. E. V. (2017). *SWAP version 4; theory description and user manual* (Report 2780). Wageningen Environmental Research. https://library.wur.nl/WebQuery/wurpubs/fulltext/416321

Leuschner, C., Weithmann, G., Bat-Enerel, B., & Weigel, R. (2023). The future of European beech in northern Germany—Climate change vulnerability and adaptation potential. *Forests*, *14*, 1448. https://doi.org/10.3390/f14071448

Marwick, B., Boettiger, C., & Mullen, L. (2017). Packaging data analytical work reproducibly using R (and friends). *PeerJ Preprints*. https://doi.org/10.7287/peerj.preprints.3192v1

Mualem, Y. (1976). A new model for predicting the hydraulic conductivity of unsaturated porous media. *Water Resources Research*, *12*(3), 513–522.

Peltier, D. M. P., Barber, J. J., & Ogle, K. (2018). Quantifying antecedent climatic drivers of tree growth in the southwestern US. *Journal of Ecology*, *106*, 613–624.

Plagge, R. (1991). *Bestimmung der ungesättigten hydraulischen Leitfähigkeit* [Doctoral thesis, Technical University]. (In German).

Rakei, A. (1991). *Wasserhaushalt eines Alt- und Jungkiefernbestandes auf Rostbraunerde des Grunewaldes* [Master's thesis, Technische Universität Berlin]. (In German).

Renger, M., & Strebel, O. (1980). Jährliche Grundwasserneubildung in Abhängigkeit von Bodennutzung und Bodeneigenschaften. *Wasser und Boden*, *32*(8), 362–366. (In German).

Riek, W., Wessolek, G., & von Lührte, A. (1994). *Wasserhaushalt und Zuwachsverhalten von Kiefern und Eichen im Raum Berlin* [Master's thesis, Bodenökologie und Bodengenese, Heft]. (In German).

Riek, W., Wessolek, G., & von Lührte, A. (1995a). Interpretation von Jahrringzeitreihen mittels Variogrammanalyse. *Dendrochronologia*, *13*, 149–154. (In German).

Riek, W., Wessolek, G., & von Lührte, A. (1995b). Wasserhaushalt und Dickenwachstum von Kiefern im Raum Berlin. *Allgemeine Forst-und Jagdzeitung*, *166*(7), 138–144. (In German).

Riek, W., Wessolek, G., & von Lührte, A. (1995c). Spektralanalytische Interpretation des langjährigen Wasserhaushalts und der Jahrringbreitenentwicklung von Kiefern (*Pinus sylvestris*). *Forstarchiv*, *66*(5), 199–205. (In German).

Rijtema, P. E. (1968). *On the relation between transpiration, soil physical properties and crop production as a basis for water supply plans* (Technical Bulletin No. 158). Institute for Land and Water Management Research.

Russ, A., Riek, W., & Martin, J. (2017). *Forstliches Umweltmonitoring Mecklenburg-Vorpommern. Ergebnisse der Untersuchungen auf den Intensivmonitoringflächen (Level II) (Heft* 10). Mitteilungen aus dem Forstlichen Versuchswesen. (In German).

Scharnweber, T., Smiljanic, M., Cruz-García, R., Manthey, M., & Wilmking, M. (2020). Tree growth at the end of the 21st century—The extreme years 2018/19 as template for future growth conditions. *Environmental Research Letters*, *15*(7), 74022. https://doi.org/10.1088/1748-9326/ab865d

Spiecker, H., & Kahle, H.-P. (2023). Climate-driven tree growth and mortality in the Black Forest, Germany—Long-term observations. *Global Change Biology*, *29*(20), 5908–5923. https://doi.org/10.1111/gcb.16897

Vacek, Z., Vacek, S., & Cukor, J. (2023). European forests under global climate change: Review of tree growth processes, crises and management strategies. *Journal of Environmental Management*, *332*(7), 117353. https://doi.org/10.1016/j.jenvman.2023.117353

van Genuchten, M. Th. (1980). A closed-form equation for predicting the hydraulic conductivity of unsaturated soils. *Soil Science Society of America Journal*, *44*, 892–898.

Veuillen, L., Prévosto, B., Alfaro-Sánchez, R., Badeau, V., Battipaglia, G., Beguería, S., Bravo, F., Boivin, T., Camarero, J. J., Čufar, K., Davi, H., De Luis, M., Del Campo, A., Del Rio, M., Di Filippo, A., Dorman, M., Durand-Gillmann, M., Ferrio, J. P., Gea-Izquierdo, G., … Cailleret, M. (2023). Pre- and post-drought conditions drive resilience of *Pinus halepensis* across its distribution range. *Agricultural and Forest Meteorology*, *339*, 109577. https://doi.org/10.1016/j.agrformet.2023.109577

von Lührte, A. (1991). *Dendro-ökologische Untersuchungen an Kiefern und Eichen in den stadtnahen Berliner Forsten*. Landschaftsentwicklung und Umweltforschung. (In German).

Von Wilpert, K. (1990). *Die Jahrringstruktur von Fichten in Abhängigkeit vom Bodenwasserhaushalt auf Pseudogley und Parabraunerde—Ein Methodenkonzept zur Erfassung standortsspezifischer Wasserstressdisposition*. Freiburger Bodenkundliche Abhandlungen, Bd. 24. Selbstverlag Institut für Bodenkunde und Waldernährungslehre der AlbertLudwigs-Universität Freiburg i. Br. (In German).

Weiß, C. (2006). *Datenanalyse und Modellierung mit STATISTICA*. Verlag Oldenburg Wissenschaft. (In German).

Wessolek, G. (1989). *Einsatz von Wasserhaushalts- und Photosynthesemodellen in der Ökosystemanalyse*. In *Landschaftsentwicklung und*

Umweltforschung No 61 (p. 170). Technische Universität Berlin. (In German).

Wessolek, G., Duijnisveld, W. H. M., & Trinks, S. (2008). Hydro-pedo-transfer-functions (HPTFs) for predicting annual percolation rate on a regional scale. *Journal of Hydrology*, *356*, 17–27.

Wessolek, G., & Kluge, B. (2021). Predicting water supply and evapotranspiration of street trees using hydro-pedo-transfer functions (HPTFs). *Forests*, *12*, 1010. https://doi.org/10.3390/f12081010

Wessolek, G., Schwärzel, K., Greiffenhagen, A., & Stoffregen, H. (2008). Percolation characteristics of a water-repellent sandy forest soil. *European Journal of Soil Science*, *59*, 14–23.

How to cite this article: Wessolek, G., Riek, W., & Bohne, K. (2024). Hydro-pedo-transfer-functions expressing drought and memory effects on pine tree growth. *Vadose Zone Journal*, *23*, e20317. https://doi.org/10.1002/vzj2.20317